

## Supplementary Information

### Architecture of SWI/SNF Chromatin Remodeling Complex

Zhihui Zhang<sup>1</sup>, Xuejuan Wang<sup>1, 2</sup>✉, Jiyu Xin<sup>1</sup>, Zhenrui Ding<sup>1</sup>, Sheng Liu<sup>1</sup>, Qianglin Fang<sup>3</sup>, Na Yang<sup>3</sup>, Rui-min Xu<sup>3</sup>, Gang Cai<sup>1, 2</sup>✉

<sup>1</sup>Hefei National Laboratory for Physical Sciences at Microscale and School of Life Sciences, University of Science & Technology of China, Hefei, Anhui, China;

<sup>2</sup>CAS Center for Excellence in Molecular Cell Science, Chinese Academy of Sciences, Hefei, 230026, China;

<sup>3</sup>National Laboratory of Biomacromolecules, Institute of Biophysics, Chinese Academy of Sciences, Beijing 100101, China.

✉Correspondence: [xuejuan@ustc.edu.cn](mailto:xuejuan@ustc.edu.cn) (X. Wang), [gcai@ustc.edu.cn](mailto:gcai@ustc.edu.cn) (G. Cai)

## MATERIALS AND METHODS

### Yeast strains

The budding yeast *Saccharomyces cerevisiae* strains that were used in this study are listed in table S1. A standard one-step polymerase chain reaction (PCR) approach was applied to generate yeast strains harboring individual gene deletions or with modified TAP (Cai et al., 2009) (10 X histidine-TEV-ProteinA) tag at the C terminus of the target protein (Knop et al., 1999). The Arp7, Arp9 and Swi1 subunit deletions are heterozygous deletions and the Snf5 and Swp82 deletion mutant are homozygous deletion. All the modifications were made in the multiple protease-deficient *S. cerevisiae* strain BJ2168 (*MATa leu2 trp1 ura3-52 prb1-1122 pep4-3 prc1-407 gal2*), except the Snf5 homozygous deletion is in the BY4742 (*MATa SWI3-TAPm snf6Δ::KanMX leu2Δ0 lys2Δ0 ura3Δ0*) and acquired from the Homozygous Diploid Complete Set (Cat. no. 95401.H1R3, Invitrogen).

### Purification of Yeast SWI/SNF.

The wild-type or subunit deletion mutant strains were grown in YPD medium to the stationary phase. About 100 g cells were harvested, washed and re-suspended in extraction buffer (50 mM HEPES (pH 7.6), 300 mM KOAc, 0.5 mM EDTA, 5 mM b-ME, 10% (v/v) glycerol, 0.1% (v/v) NP-40 and protease inhibitors), and a whole-cell extraction was prepared as previously described (Takagi et al., 2005). This whole-cell extract was selectively precipitated in 30–55% ammonium sulfate and resuspended using 1xTEZ buffer (50 mM Tris-HCl (pH 7.5), 1 mM EDTA, 10 mM ZnCl<sub>2</sub>, 5 mM b-ME and protease inhibitors). After the suspension was clarified using centrifugation, the supernatant was incubated for 2 h at 4 °C with 1 ml of a 50% slurry of IgG-sepharose resin beads (GE Healthcare) that had been pre-equilibrated with 1xTEZ plus 250 mM ammonium sulfate. After incubation, the beads were washed with 50 ml of 1xTEZ plus 500 mM ammonium sulfate, followed by a second wash with 50 ml of 11xTEZ plus 50 mM ammonium sulfate. After equilibration of the column with 1xTEZ plus 100 mM ammonium sulfate (without protease inhibitors), 100 units of AcTEV protease

(Invitrogen) was added to the resin beads and incubated overnight at 4 °C. The SWI/SNF fraction was then eluted with three column volumes of 1xTEZ plus 100 mM ammonium sulfate and 10% glycerol was added, and the resulting aliquot was snap-frozen in liquid nitrogen and temporarily stored at -80 °C. For the next purification step, the IgG eluate fractions were thawed in ice and applied on a Mono S column (GE Healthcare) in S100 buffer (100mM ammonium sulfate, 50mM Tris pH 7.6, 10% vol/vol glycerol, 1mM EDTA, 10 $\mu$ M ZnSO<sub>4</sub>, 0.02% NP-40, 10mM  $\beta$ -ME) and was resolved over a 100–1000 mM ammonium sulfate gradient. The final SWI/SNF fractions eluted at ~400mM ammonium sulfate concentration were flash-frozen in liquid nitrogen.

### **Assembly of the SWI/SNF-Nucleosome complex**

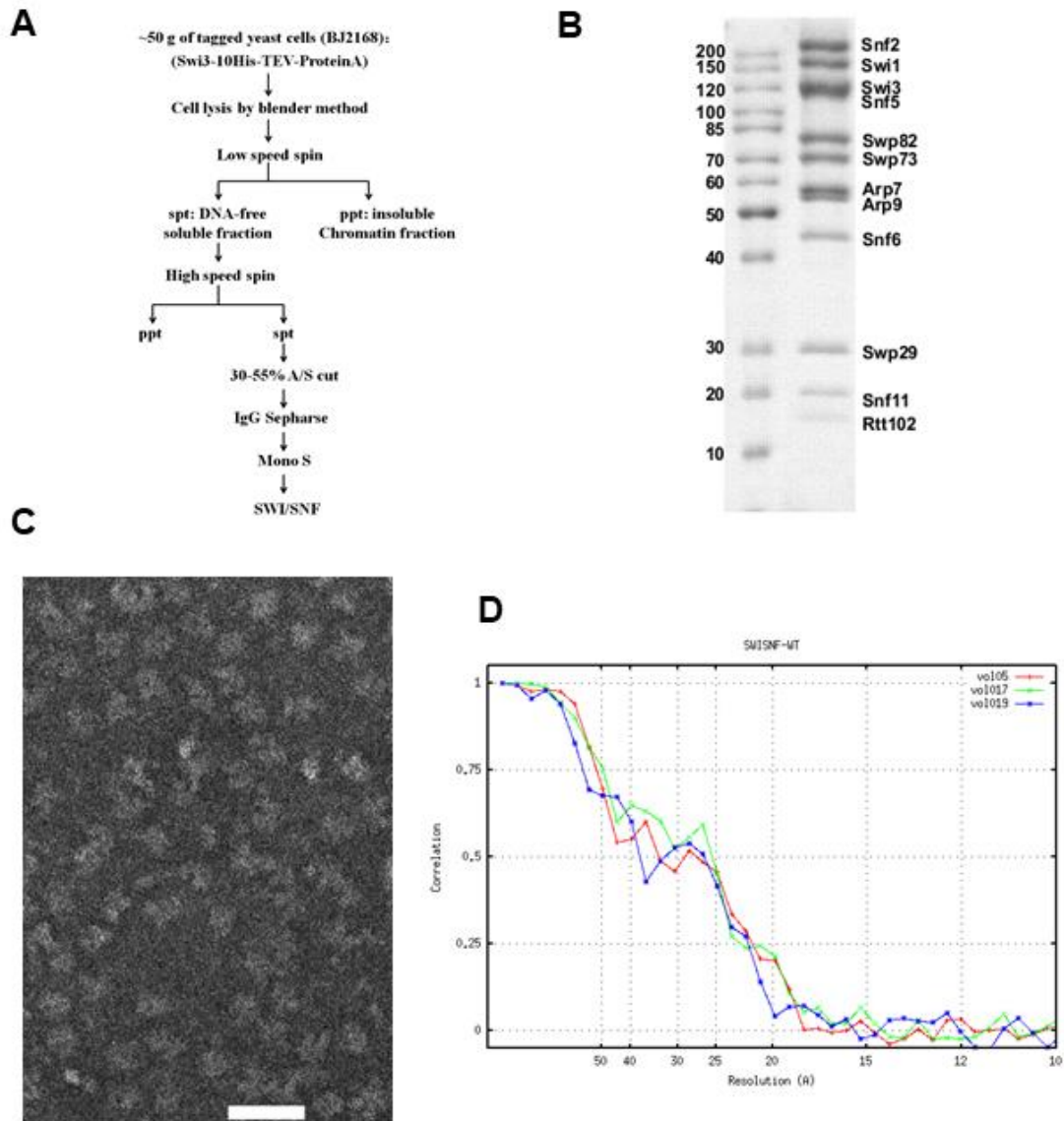
NCP made of bacterially expressed *S. cerevisiae* histones H2A, H2B, H3 and H4 and a 146-bp palindromic DNA fragment derived from human  $\alpha$ -satellite DNA was prepared according to a described procedure (Luger et al., 1997b). The Mono S peak fraction of the SWI/SNF was incubated with Ni-NTA resin (Quigen) that had been pre-equilibrated with buffer A (20 mM Hepes (pH 7.9), 125 mM NaCl, 2.5 mM MgCl<sub>2</sub>, 1 mM DTT and 2.6% glycerol), then washed with buffer A. After equilibration of the column with buffer B (20 mM Hepes(pH 7.9), 125 mM NaCl, 2.5 mM MgCl<sub>2</sub>, 1 mM DTT, 1mM ATP $\gamma$ S, and 2.6% glycerol), 400pmol nucleosome core particles was added and incubated for 2 hour at 4°C, then was chemical crosslinked with final concentration of 0.04% glutaraldehyde for 5 min under room temperature and quenched the crosslinking with buffer A washing. The SWI/SNF-Nucleosome assembly was eluted with buffer C (20 mM Hepes (pH 7.9), 125 mM NaCl, 2.5 mM MgCl<sub>2</sub> , 1 mM DTT, 250mM imidazole, and 2.6% glycerol). The resulting aliquot was snap-frozen in liquid nitrogen and temporarily stored at -80 °C.

### **Negative stain reconstruction**

About 3 $\mu$ L sample aliquots (~30  $\mu$ g protein/ml in 50mM Tris pH 7.6, 100mM

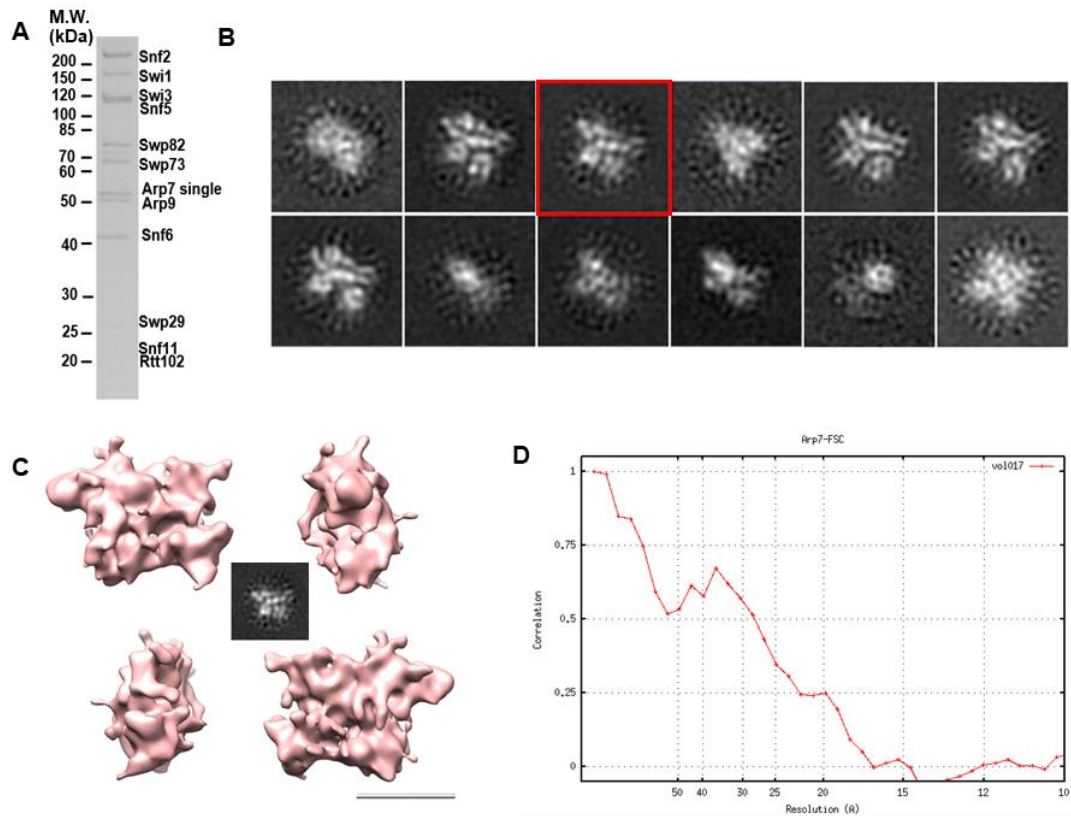
ammonium sulfate, 10% vol/vol glycerol, 1mM EDTA, 10 $\mu$ M ZnSO<sub>4</sub>, 0.02% NP-40, 10mM  $\beta$ -ME) was applied to a carbon-coated 300-mesh Cu EM specimen grid freshly glow discharged. The SWI/SNF particles were then preserved by staining with 0.75 % (w/w) uranyl formate solution. The particles of the SWI/SNF show a strongly preferred orientation on adsorption to amorphous carbon support films. To obtain the initial model for cryo-EM refinement, 3D reconstructions were calculated by using the RCT method (Radermacher, 1988)

We obtained tilted (55°) and untilted image pairs of SWI/SNF particles under low-dose conditions using a Tecnai F20 microscope (FEI) (field emission gun, low-dose conditions, 200-kV accelerating voltage, ~0.6 to 0.8  $\mu$ m under focus). Images were recorded with a FEI Eagle (4k HS 200kv) CCD camera at 62,000 $\times$  magnification (1.77 Å per pixel) and two-fold pixel-averaged to 3.54 Å per pixel. Particles were selected using the TiltPicker program (Voss et al., 2009) and montaged them for interactive screening, yielding ~9,000 single particle tilt-pair images. We run iterative alternating rounds of supervised multi-reference alignment and classification as well as reference-free alignment to improve the homogeneity of the image classes. All the 3D reconstructions were calculated with SPIDER (Frank et al., 1996) and SPARX (Hohn et al., 2007). All the 3D structures were displayed using Chimera (Pettersen et al., 2004).



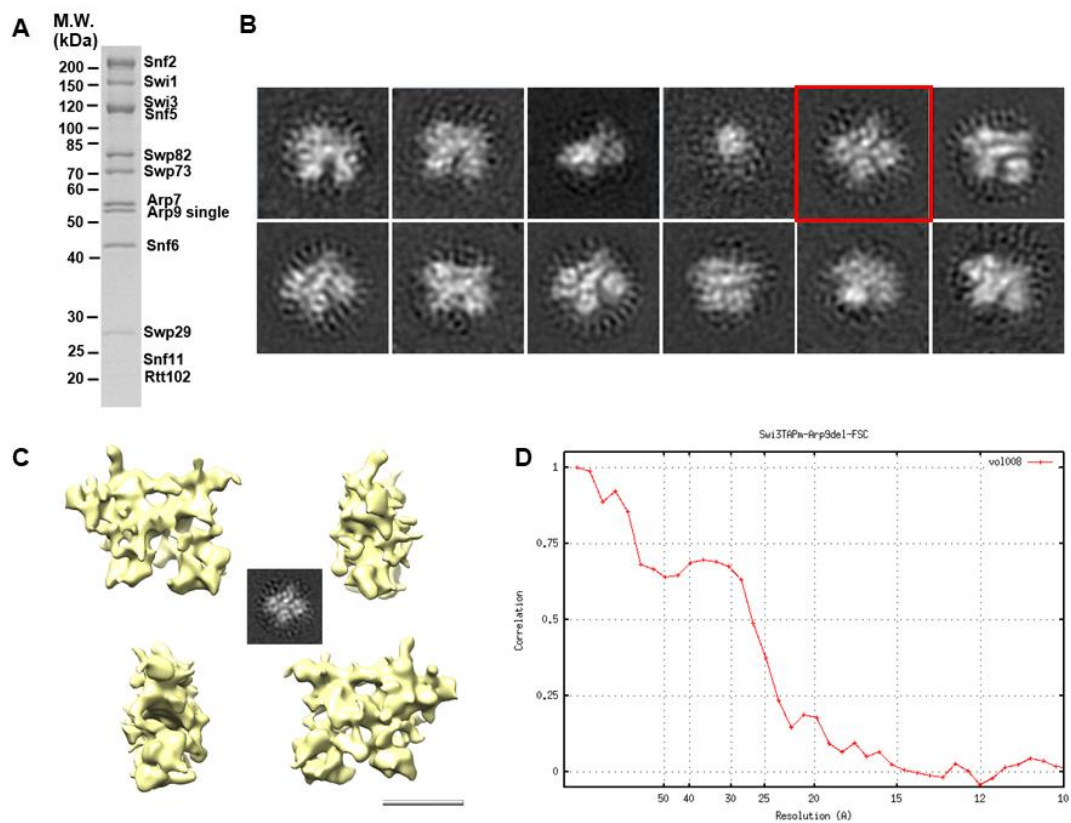
**Supplementary Figure 1. EM reconstruction of the intact SWI/SNF complex.**

(A) Scheme for affinity purification of SWI/SNF complex from the whole cell extraction of tagged *S. cerevisiae* cells. (Abbreviations: spt, supernatant; ppt, precipitation.) (B) The SDS-PAGE analysis of the 12-subunit SWI/SNF complex. (C) A micrograph showing single SWI/SNF particles preserved under stain. Scale bar, 50 nm. (D) Fourier Shell Correlation (FSC) curve for the RCT reconstruction. Using a FSC = 0.5 criterion, the resolution of the maps are estimated to be ~25~38 Å.



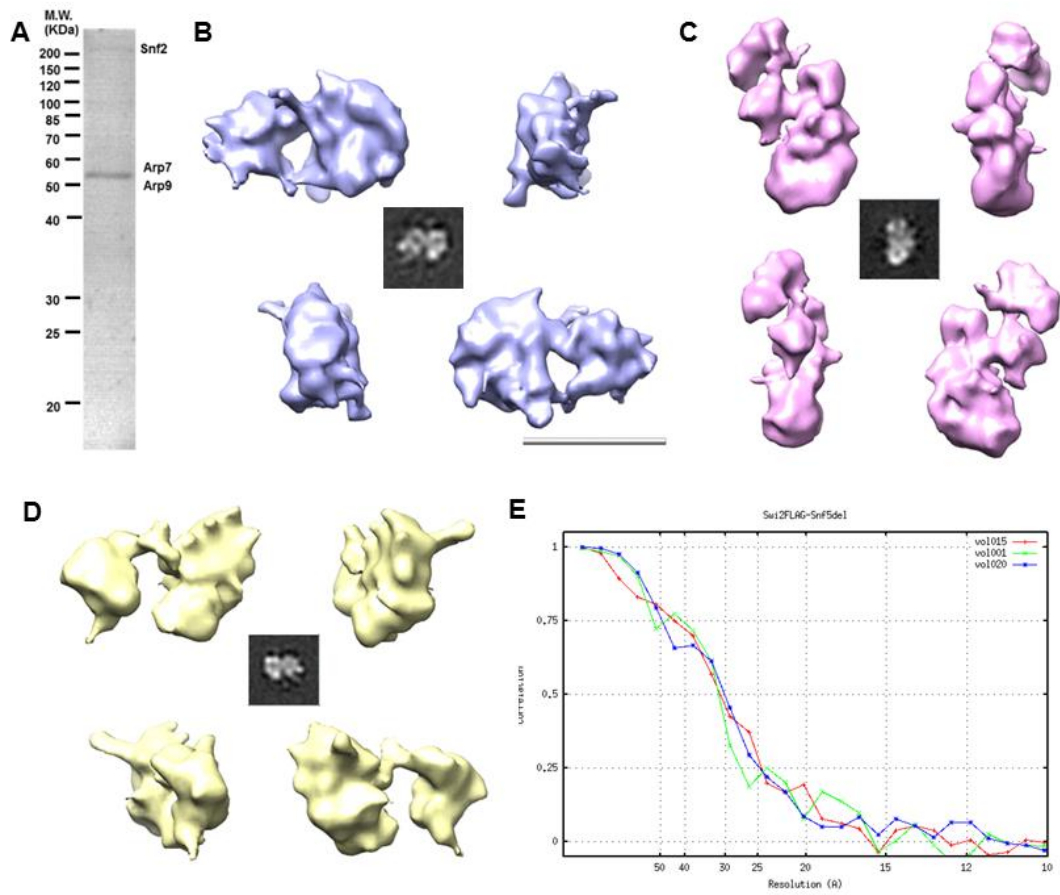
**Supplementary Figure 2. EM reconstruction of the SWI/SNF subcomplex purified from Arp7 deletion strain.**

(A) Ruby-stain SDS-PAGE analysis of the subcomplex endogenously purified from the *S.cerevisiae* Arp7 $\Delta$  strain. (B) 2D averages of the SWI/SNF subcomplex from the Arp7  $\Delta$  strain. Red square represents the class used in further analysis. (C) 2D and 3D EM analysis of the subcomplex from the Arp7 $\Delta$  strain. Scale bar, 100 Å. (D) Fourier Shell Correlation (FSC) curve for the RCT reconstruction of the Arp7 $\Delta$  subcomplex. Using a FSC = 0.5 criterion, the resolution of the map is estimated to be ~28 Å.



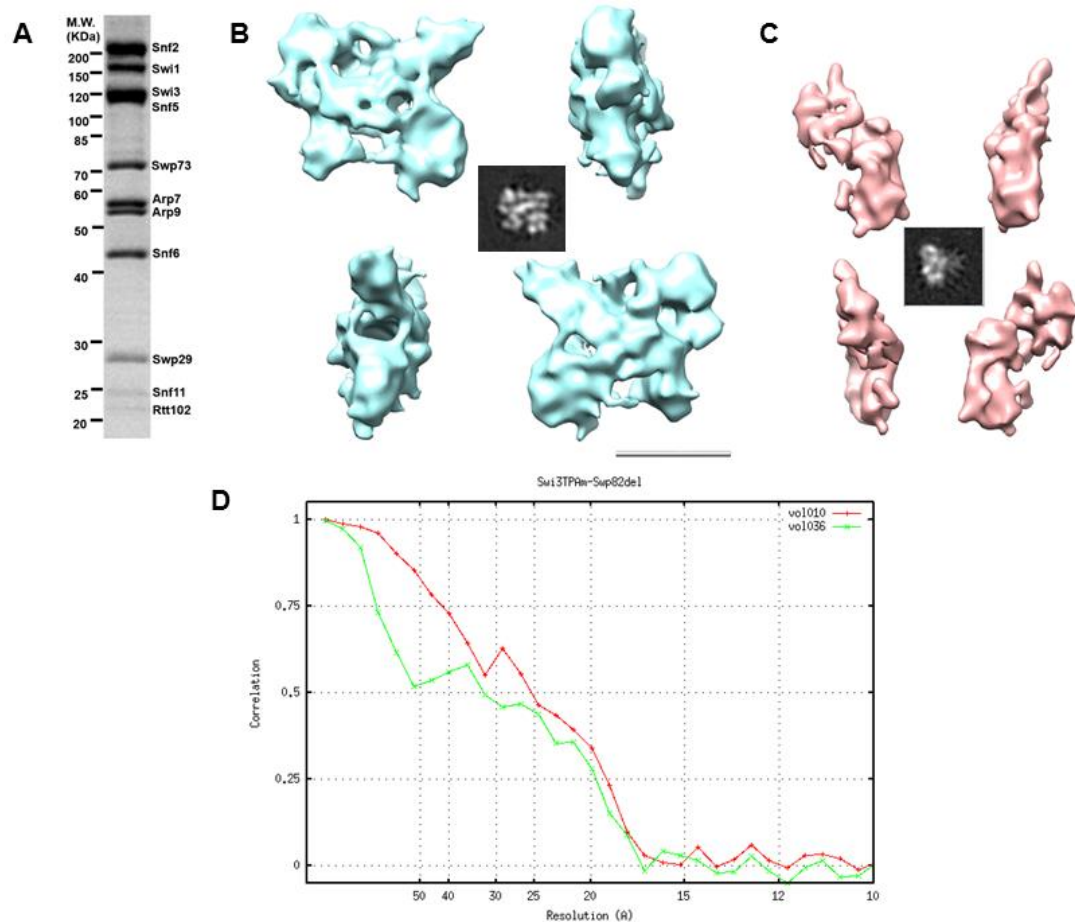
**Supplementary Figure 3. EM reconstruction of the SWI/SNF subcomplex purified from Arp9 deletion strain.**

(A) Ruby-stain SDS-PAGE analysis of the subcomplex endogenously purified from the *S.cerevisiae* Arp9 $\Delta$  strain. (B) 2D averages of the SWI/SNF subcomplex from the Arp9  $\Delta$  strain. Red square represents the class used in further analysis. (C) 2D and 3D EM analysis of the subcomplex from the Arp9 $\Delta$  strain. Scale bar, 100 Å. (D) Fourier Shell Correlation (FSC) curve for the RCT reconstruction of the Arp9 $\Delta$  subcomplex. Using a FSC = 0.5 criterion, the resolution of the map is estimated to be ~24 Å.



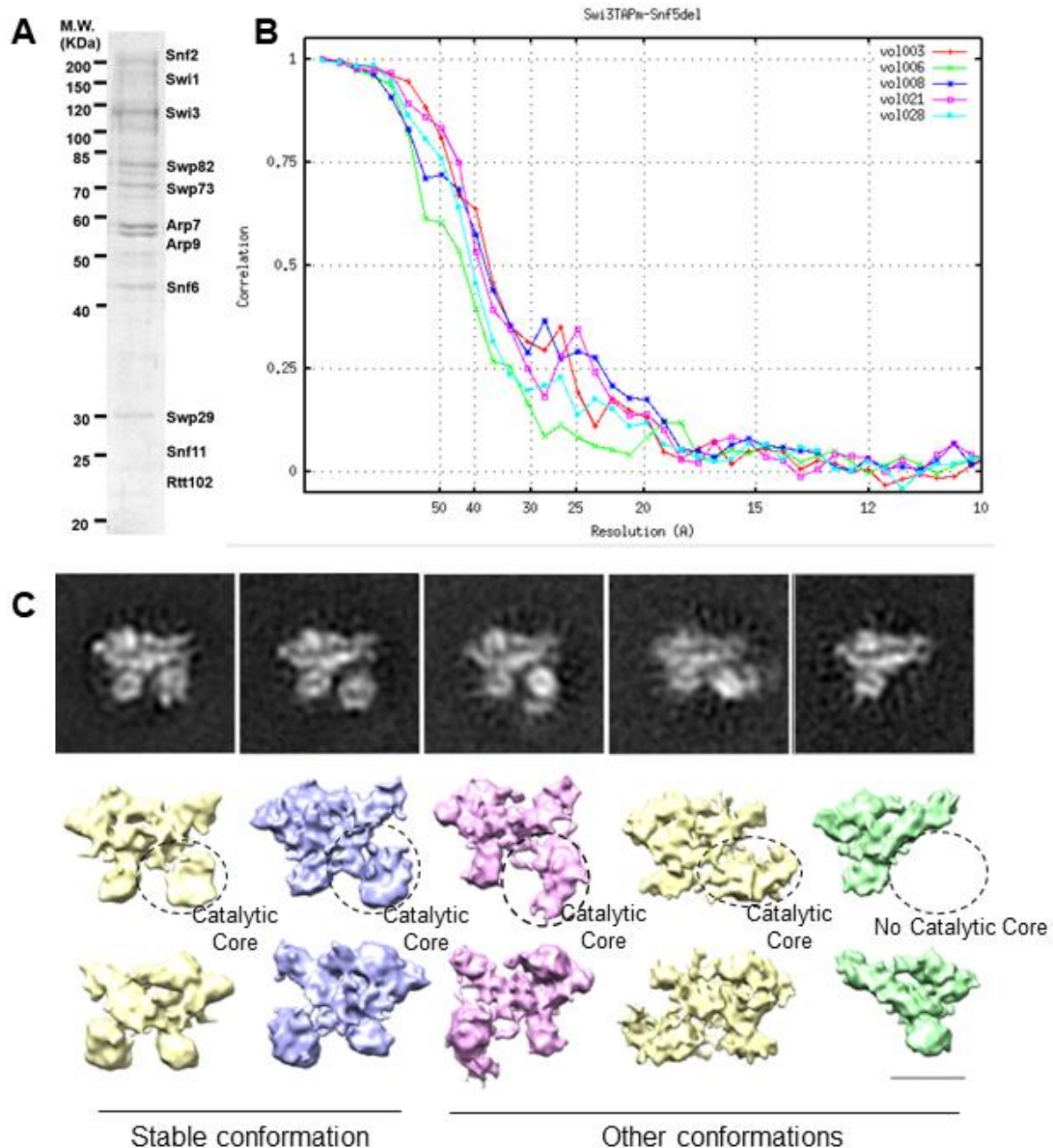
**Supplementary Figure 4. EM reconstruction of the catalytic core subcomplex purified from the Snf2-FLAG/Snf5 $\Delta$  strain.**

(A) Ruby-stain SDS-PAGE analysis of the catalytic core subcomplex containing Snf2, Arp7 and Arp9. (B, C, D) 2D and 3D EM analysis of the three conformations of the catalytic core subcomplex. Scale bar, 100 Å. (E) Fourier Shell Correlation (FSC) curve for the RCT reconstruction. Using a FSC = 0.5 criterion, the resolution of the maps are estimated to be ~30 Å.



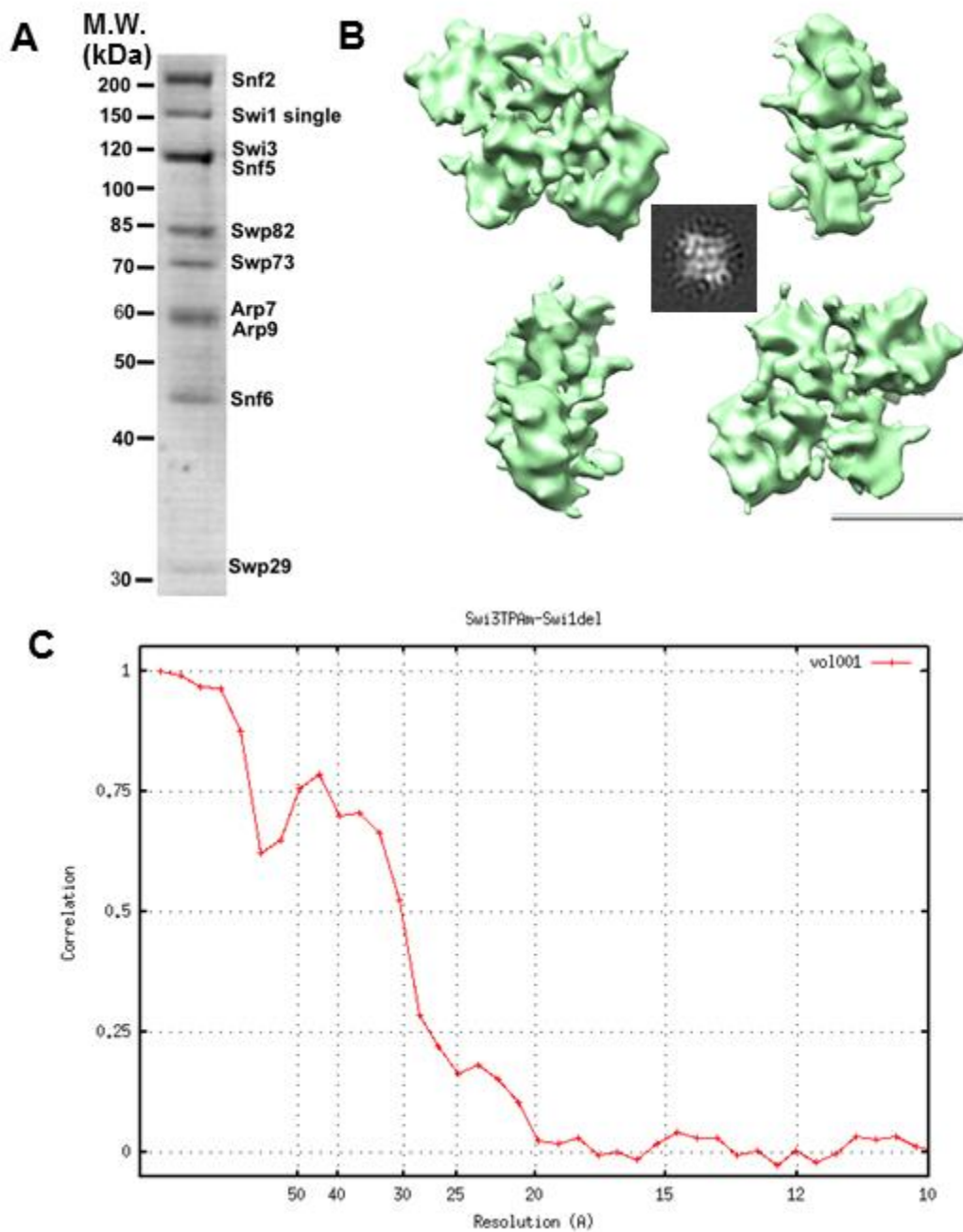
**Supplementary Figure 5. EM reconstruction of the SWI/SNF subcomplex purified from *S. cerevisiae* Swp82 $\Delta$  strain.**

(A) Ruby-stain SDS-PAGE analysis of the subcomplex endogenously purified from the *S. cerevisiae* Swp82 $\Delta$  strain. (B, C) 2D and 3D EM analysis of the two subcomplex from the Swp82 $\Delta$  strain. Scale bar, 100 Å. (D) Fourier Shell Correlation (FSC) curve for the RCT reconstruction of the Swp82 $\Delta$  subcomplex. Using a FSC = 0.5 criterion, the resolution of the maps are estimated to be ~25~32 Å.



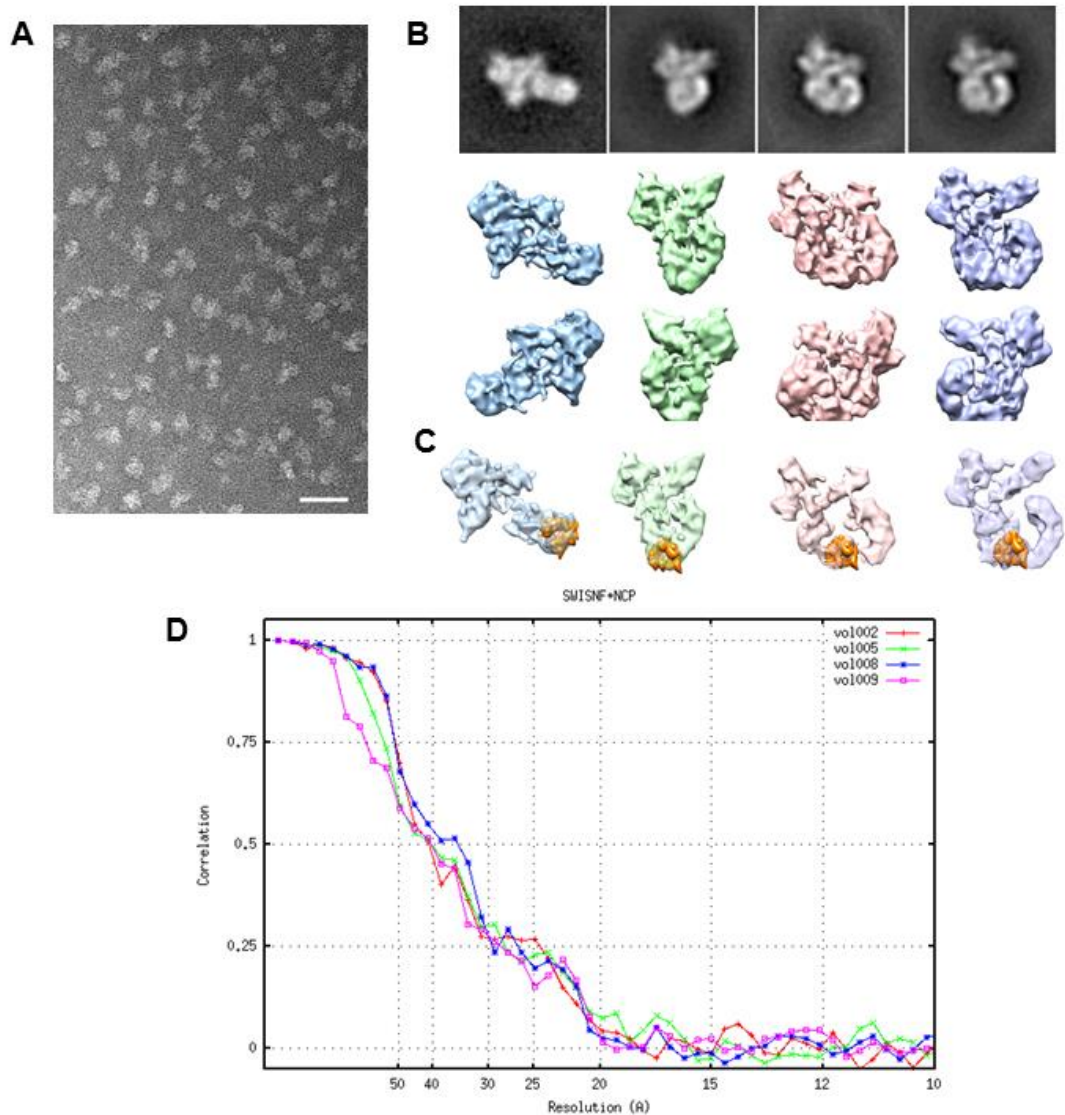
**Supplementary Figure 6. EM reconstruction of the subcomplex purified from *S. cerevisiae* Snf5 $\Delta$  strain.**

(A) Ruby-stain SDS-PAGE analysis of the subcomplex endogenously purified from the *S. cerevisiae* Snf5 $\Delta$  strain. (B) Fourier Shell Correlation (FSC) curve for the RCT reconstruction of the Snf5 $\Delta$  subcomplex. Using a FSC = 0.5 criterion, the resolutions of the maps are estimated to be ~37~42 Å. (C) 2D and 3D EM analysis of the subcomplex from the Snf5 $\Delta$  strain. At least six different conformations were identified through reference-free alignment and classification of EM images. Distinct structures of the Snf5 deletion mutant. The mobility of the catalytic core is substantially boosted in the absence of the Snf5 subunit, which even could be fully detached. Scale bar, 100 Å.



**Supplementary Figure 7. EM reconstruction of the subcomplex purified from *S. cerevisiae* Swi1 heterozygous deletion strain.**

(A) Ruby-stain SDS-PAGE analysis of the subcomplex endogenously purified from the *S. cerevisiae* Swi1 $\Delta$  strain. (B) 2D and 3D EM analysis of the subcomplex from the Swi1 $\Delta$  strain. Scale bar, 100 Å. (C) Fourier Shell Correlation (FSC) curve for the RCT reconstruction of the Swi1 $\Delta$  subcomplex. Using a FSC = 0.5 criterion, the resolution of the map is estimated to be ~30 Å.



**Supplementary Figure 8. EM reconstructions of the four nucleosome binding states of the SWI/SNF.**

(A) A micrograph showing single particles of the SWI/SNF binding a nucleosome preserved under stain. Scale bar, 50 nm. (B) 2D and 3D EM analysis of the four states. (C) 3D maps of the four nucleosome binding states showing at the lower density threshold with the bound nucleosomes highlighted by solid orange densities. (D) Fourier Shell Correlation (FSC) curves for the RCT reconstruction of the complex. Using a FSC = 0.5 criterion, the resolution of the maps are estimated to be ~34~40 Å.

## Supplementary Table 1

### Yeast strains used in this study.

Strains	Genotype	Genetic Background
SWI3-TAPm	<i>MATa SWI3-TAPm leu2 ura3-52 prb1-1122 pep4-3 prc1-407 gal2</i>	BJ2168
SWI3-TAPm-ARP9 $\Delta$ *	<i>MATa SWI3-TAPm arp9<math>\Delta</math>:: KanMX leu2 ura3-52 prb1-1122 pep4-3 prc1-407 gal2</i>	BJ2168
SWI3-TAPm-ARP7 $\Delta$ *	<i>MATa SWI3-TAPm arp7<math>\Delta</math>:: KanMX leu2 ura3-52 prb1-1122 pep4-3 prc1-407 gal2</i>	BJ2168
SWI3-TAPm-SWP82 $\Delta$	<i>MATa SWI3-TAPm swp82<math>\Delta</math>:: KanMX leu2 ura3-52 prb1-1122 pep4-3 prc1-407 gal2</i>	BJ2168
SWI3-TAPm-SWI1 $\Delta$ *	<i>MATa SWI3-TAPm swi1<math>\Delta</math>:: KanMX leu2 ura3-52 prb1-1122 pep4-3 prc1-407 gal2</i>	BJ2168
SWI3-TAPm-SNF5 $\Delta$	<i>MATa SWI3-TAPm snf5<math>\Delta</math>:: KanMX leu2<math>\Delta</math>0 lys2<math>\Delta</math>0 ura3<math>\Delta</math>0</i>	BY4742
SNF2-FLAG-SNF5 $\Delta$	<i>MATa SNF2-FLAG snf5<math>\Delta</math>:: KanMX leu2<math>\Delta</math>0 lys2<math>\Delta</math>0 ura3<math>\Delta</math>0</i>	BY4742

**Note:** \* represents heterozygous deletions